Supporting Information:

High fluence electrospray ionization

The large trapping volume of the NanoClusterTrap cannot be used to full capacity with standard electrospray ionization (ESI) sources. To facilitate delivery of sufficient $(melittin+qH)^{q+}$ ion current, we have developed a high intensity ESI source (for a sketch, see Fig.).

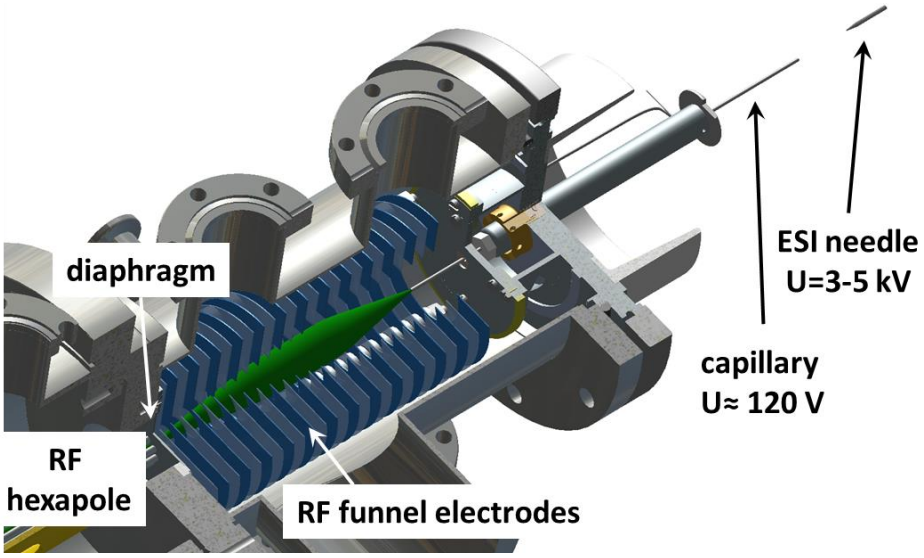

Fig. S1: Sketch of the electrospray ionionization source. The needle and capillary entrance operate under atmospheric pressure and the pressure in the RF funnel is $5x10^{-1}$ mbar.

Melittin ($C_{131}H_{229}N_{39}O_{31}$, Sigma-Aldrich) was dissolved into a 35 µM concentration consisting of a mixture of 55% methanol and 45% water in volume. 1% of formic acid was added to the solution in order to facilitate protonation. The solution was sprayed under atmospheric pressure towards a capillary, heated to approximately 373 K. The needle was biased to 3 kV. Positively charged microdroplets are formed in the spraying process, which are subject to cycles of evaporation and Coulomb explosion, until the desired free $(melittin+qH)^{q+}$ ions are formed. After passing the capillary, the ions were phase space compressed by means of a radiofrequency ion funnel, operating at a background pressure of about $5x10^{-1}$ mbar. The ions were then transported to a radiofrequency hexapole ion guide through a 2 mm diaphragm. The ion current delivered by the source crucially depends on both capillary inner diameter and exit diaphragm diameter.

To maximize the delivered ion current, a very large inner diameter of the heated capillary (0.76 mm) was chosen. Using a 250 m^3/h roots blower pump, despite the large capillary diameter, typical pressures in the funnel region of $2\text{-}5x10^{-1}$ mbar could be achieved. With funnel frequencies of 240-320 kHz and amplitudes of 250-300V, the source produced total ion currents of up to 1 nA with typical ion currents of mass selected protonated melittin cations of 100-200 pA.

Coupling to the Nanoclustertrap setup

The high fluence ESI source was interfaced with the hexapole radiofrequency ion guide of the Nanoclustertrap apparatus. Briefly, the electrosprayed proteins ions where then mass selected using a radiofrequency quadrupole mass filter and continuously transported into a

linear radiofrequency ion trap. The ion trap content was overlapped with a soft X-ray beam from the UE52-PGM beamline of the BESSY II synchrotron at Helmholtz Zentrum Berlin, Germany. By means of a pulsed extraction, trapped ions were transported into a reflectron type time of flight mass spectrometer. The monochromator was set to an energy resolution of 250 meV and the photon energy was then scanned from 280 eV to 300 eV in steps of 125 meV. Typical acquisition periods per energy interval were 8s at photon fluences generally exceeding $5x10^{12}$/s. Typical TOF spectra are displayed in Figure S1. At least two datasets of the displayed type were accumulated for extraction of a spectrum. We recorded the data repeatedly during 2 different beamtimes and found reproducible spectra. Note, that fragmentation into sequence ions and immonium ions is not investigated in the article.

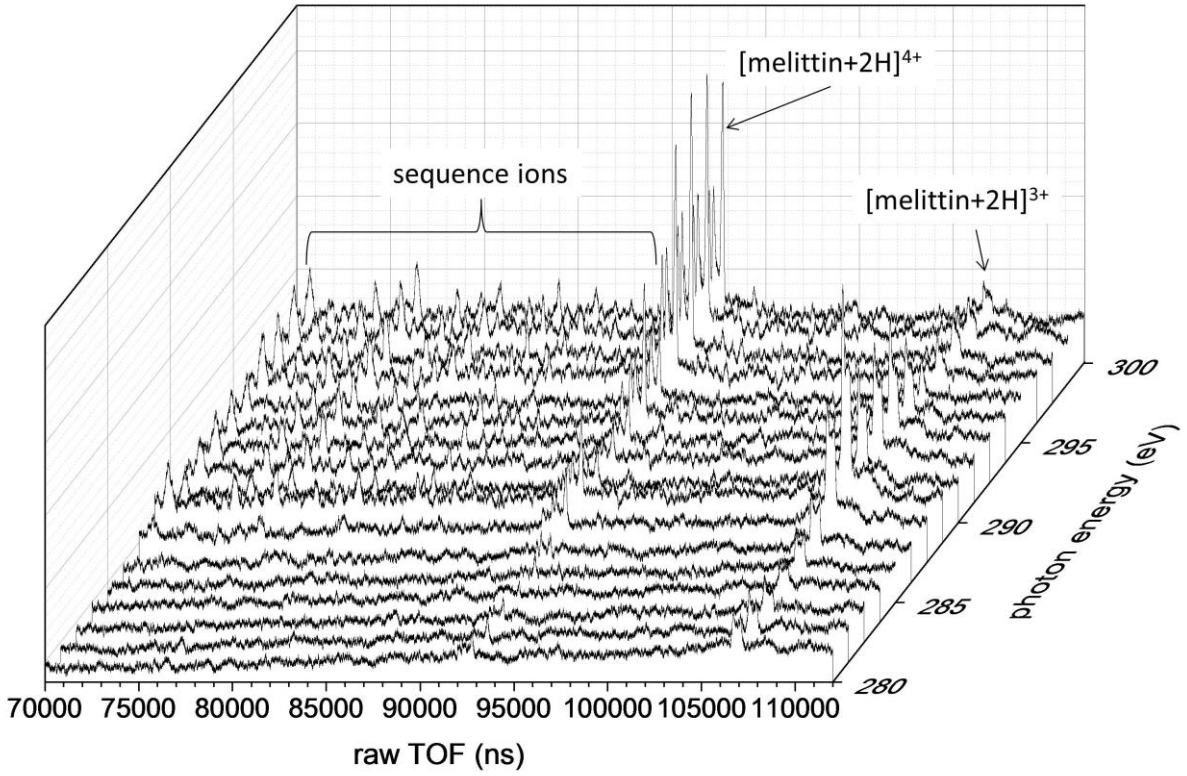

Figure S1 A sample of raw TOF spectra obtained for a a C K-edge scan of $[melittin+2H]^{2+}$. Only every 10th TOF trace is displayed. The spectra displayed in Figs. 1 and 2 of the article were obtained by integration of the single ionization $[melittin+2H]^{3+}$ and the double ionization $[melittin+2H]^{4+}$ peaks, after careful background subtraction.

Time-dependent density function theory calculations

Generally, the strength of a resonant transition is characterized by the oscillator strength between the initial 1s state and the final state. In the dipole approximation, the oscillator strength is proportional to the transition dipole moment:

$$f_{OS} \propto \left| e\langle \Psi_{final} | \boldsymbol{r} | \Psi_{1s} \rangle \right|^2 \propto \left| e \int \Psi^*_{final} \mathbf{r} \Psi_{1s}\, dV \right|^2$$

Here, Ψ_{1s} and Ψ_{final} are the wave functions of the C 1s orbital and of the carbonyl π* orbital, **r** is the position operator and e is the electron charge. The integral represents the overlap

between the two states. α-helical structure in proteins is stabilized by hydrogen bonds between the amide C=O group and the amide N-H group, four residues later in the sequence. Hydrogen bond formation can alter the nature of molecular orbitals in the groups involved and therefore influences oscillator strengths. To fundamentally understand the effect of hydrogen bonding on C 1s-π* transition probabilities for the case of an α-helical structure, we have employed a model peptide consisting of 8 glycine residues. The Avogadro program package was used to generate two Gly_8 structures with a straight chain and an α-helical backbone, respectively. To obtain the Gly8 β-hairpin structure, the Trpzip2 backbone (1LE1) [1] was used as a starting point from which all side chains were eliminated. All three model structures are displayed in Fig. S2. The structures were optimized using the Universal Force Field (UFF) [2]. Then the X-ray absorption from the 1s carbonyl carbon atoms to the carbonyl π^* orbitals was calculated using the Orca *ab initio* package [3, 4].

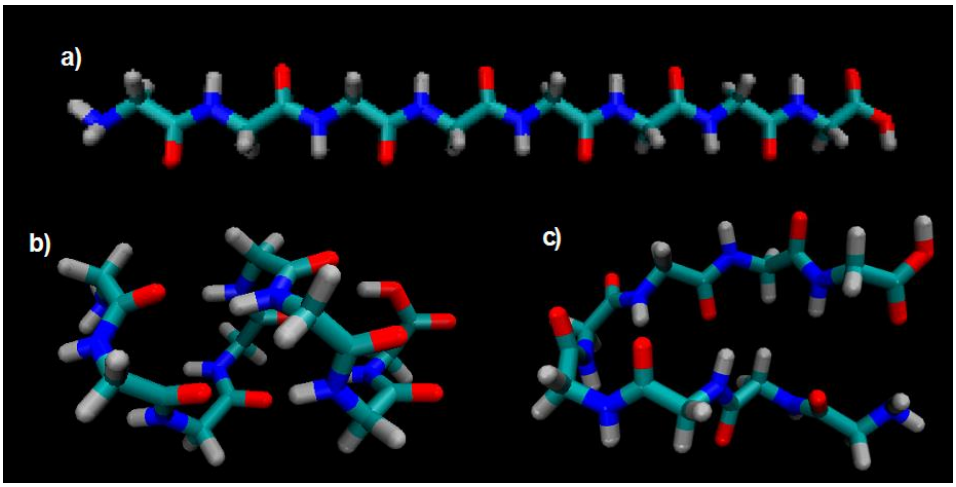

Fig. S2: The Gly_8 structures used for the electronic structure calculations (C: cyan, H: white, O: red, N: blue). a) The straight chain structure (N-terminus left, C-terminus right). b) The α-helical structure (side view, N-terminus left, C-terminus right). c) The β-hairpin structure seen from the top. The figure was rendered using the VMD package**.**

The time-dependent density functional theory (TD-DFT) [5, 6] procedure described in [7] was employed using the B3LYP [8, 9] exchange correlation functional, and the double-zeta force field with polarization (DZP) [10]. We invoked the sudden approximation dictating that the excitations occur from local carbonyl carbon 1s orbitals into the lowest valence (π*) orbitals. The excitations were calculated by demanding the excitation to be from one specific core level and repeating the calculation for all 8 core levels representing the 1s orbitals of carbonyl carbon. The calculated transition probabilities (f_{os}) included the electric, magnetic dipoles and the electric quadrupole [11], the latter two contributions were found to be minor. The results for the different conformations are summarized in **Error! Reference source not found.**. The absolute energies exhibit the commonly observed offset which depends on the choice of basis-sets and exchange-correlation functional and relative differences between the different conformations can be trusted. It is clear that for α-helix and β-hairpin, transition energies are systematically lower (up to ~0.3 eV) as compared to the linear chain reference. An exception is the C-terminus group, where energies are found to be 0.1 eV higher. Experimentally, from the spectrum in **Error! Reference source not found.**, a slightly weaker a shift of ~0.15 eV can be deduced. More importantly, the transition probabilities for all sites are smaller for the helix (with a minimum f_{os}=0.0479 for residue 6) than for the linear chain (f_{os} =0.0607 for

residue 6). For the N-terminal site the difference is marginal, but for the other sites the difference ranges from 7 to 26% reduction.

Table 1 Transition energies and intensities for the carbonyl carbon 1s to π^* transitions numbered from the N- to the C-terminal end, as obtained by time-dependent density functional theory for the geometries shown in **Error! Reference source not found.**. For the C-terminal site a closely lying transition discussed in the text is included for the α-helix structure. The reported ratio for the C-terminal is considering both transitions on the α-helix.

Chain			α-helix			β-hairpin		
site	E (eV)	f_{os}	E(eV)	f_{os}	intensity ratio	E(eV)	f_{os}	intensity ratio
1	277.63	0.0589	277.48	0.0585	1.006	277.46	0.0583	1.010
2	277.78	0.0608	277.48	0.0569	1.069	277.52	0.0575	1.058
3	277.79	0.0606	277.48	0.0561	1.080	277.42	0.0586	1.034
4	277.79	0.0606	277.47	0.0547	1.108	277.45	0.0555	1.091
5	277.79	0.0606	277.44	0.0496	1.223	277.68	0.0593	1.023
6	277.79	0.0607	277.50	0.0479	1.268	277.67	0.0623	0.974
7	277.79	0.0610	277.48	0.0504	1.21	277.49	0.0576	1.060
8	278.14	0.0655	277.89	0.0424	1.078	277.78	0.0611	1.073
8’	-	-	277.88	0.0184	-			

On the C-terminal site of the α-helix, the oscillator strength splits as two closely lying π states contribute: The acidic hydrogen is hydrogen bonding to site 5, reflecting the a-helix structure and an additional partial double-bond exists with the oxygen. For the β-hairpin the variation between the sites is larger both for the transition energies and transition probabilities. This can easily be understood as the hairpin contains a turn and there are, thus, many different types of sites. The transition probabilities are again smaller than for the straight chain, but the largest difference is only 9%, which is for a unit in the turn.

The reason for the decrease can be understood by a closer look into the transition densities for a carbonyl C atom located within the helix. In Error! Reference source not found. the respective difference and transition densities for the carbonyl of the 5^{th} glycine residue are illustrated for the three peptide structures. The observed difference is quite small, however, for the α-helix the backbone structure is distorted in a way that breaks the symmetry between the positive and negative lobes in the transition density. This distortion is paired with the lowering of the transition dipole and links the observed change intensity change of the X-ray absorption spectrum of the α-helix with an out-of-plane distortion of the backbone arising from the non-planar hydrogen bonding structure.

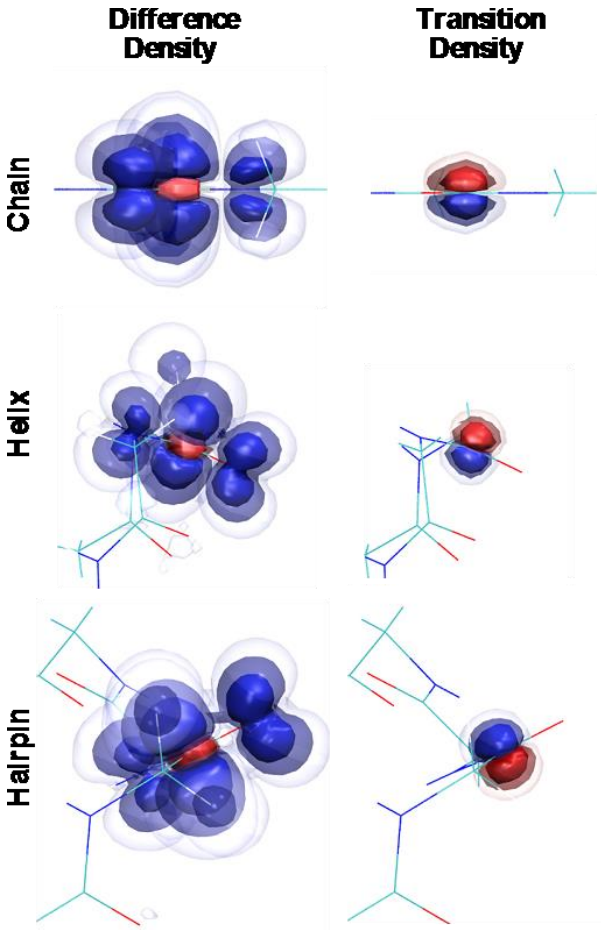

Fig. S3: The difference density and transition densities plotted for the excitation from the carbonyl carbon 1s orbital into the carbonyl $\pi*$ orbital on the fifth carbonyl. In the difference density plots the red sphere illustrates the disappearance of electron density from the 1s orbital, while the blue surfaces illustrate the electron density increase in the π^* orbital. The transition density is essentially the product of the 1s orbital and the π^* orbital.

References and Notes:

[1] A. Cochran, N. Skelton, M. Starovasnik, *Proc. Natl. Acad. Sci. U. S. A.* **2002**, *99*, 9081-9081.

[2] A. K. Rappe, C. J. Casewit, K. S. Colwell, W. A. Goddard, W. M. Skiff, *J. Am. Chem. Soc.* **1992**, *114*, 10024-10035.

[3] F. Neese, *Wiley Interdisciplinary Reviews-Computational Molecular Science* **2012**, *2*, 73-78.

[4] F. Neese, G. Olbrich, *Chemical Physics Letters* **2002**, *362*, 170-178.

[5] E. Runge, E. K. U. Gross, *Phys. Rev. Lett.* **1984**, *52*, 997-1000.

[6] S. van Gisbergen, F. Kootstra, P. Schipper, O. Gritsenko, J. Snijders, E. Baerends, *Physical Review A* **1998**, *57*, 2556-2571.

[7] S. D. George, T. Petrenko, F. Neese, *J. Phys. Chem. A* **2008**, *112*, 12936-12943.

[8] A. D. Becke, *J. Chem. Phys.* **1993**, *98*, 5648-5652.

[9] P. J. Stephens, F. J. Devlin, C. F. Chabalowski, M. J. Frisch, *J. Phys. Chem.* **1994**, *98*, 11623-11627.

[10] A. Schafer, H. Horn, R. Ahlrichs, *J. Chem. Phys.* **1992**, *97*, 2571-2577.

[11] S. D. George, T. Petrenko, F. Neese, *Inorg. Chim. Acta* **2008**, *361*, 965-972.